Synthesis and Structures of Gallium Alkylthiolate Compounds

Seigi Suh,[†] Jon H. Hardesty,[‡] Thomas A. Albright,*[,‡] and David M. Hoffman*[,†]

Department of Chemistry and the Materials Research Science and Engineering Center, University of Houston, Houston, Texas 77204

Received November 13, 1998

Gallium alkylthiolate complexes have been prepared from gallium amide complexes and thiols. The amide complex $[Ga(NMe_2)_3]_2$ reacts with excess *t*-BuSH to give the amine adduct $Ga(S\text{-}t\text{-}Bu)_3(HNMe_2)$. In contrast, the bulky amide complex $Ga(N\text{-}i\text{-}Pr_2)_3$ reacts with *t*-BuSH to give the homoleptic thiolate dimer $[Ga(S\text{-}t\text{-}Bu)_3]_2$. The analogous reaction between $Ga(N\text{-}i\text{-}Pr_2)_3$ and *i*-PrSH produces the salt $[i\text{-}Pr_2NH_2][Ga(S\text{-}i\text{-}Pr)_4]$, which on heating under vacuum loses amine and thiol to give the dimer $[Ga(S\text{-}i\text{-}Pr)_3]_2$. Reactions of $[i\text{-}Pr_2NH_2][Ga(S\text{-}i\text{-}Pr)_4]$ and $[Ga(S\text{-}t\text{-}Bu)_3]_2$ with excess pyridine give the adducts $Ga(SR)_3(py)$ (R = *i*-Pr or *t*-Bu). X-ray crystallographic studies show that the dimers have two bridging thiolate ligands. The $Ga(\mu\text{-}SR)_2Ga$ four-membered ring in $[Ga(S\text{-}i\text{-}Pr)_3]_2$ has a planar anti geometry while the ring in $[Ga(S\text{-}t\text{-}Bu)_3]_2$ has a butterfly syn configuration. In the solid state, $Ga(S\text{-}t\text{-}Bu)_3(HNMe_2)$ and $[i\text{-}Pr_2NH_2][Ga(S\text{-}i\text{-}Pr)_4]$ have trigonal-pyramidal and distorted tetrahedral geometries, respectively. The $[Ga(SR)_3]_2$ compounds exhibit solution fluxional behavior consistent with two separate processes, bridge-terminal thiolate exchange and effective inversion at the bridging sulfur atoms. Ab initio molecular orbital calculations on $[Ga(SH)_2(\mu\text{-}SH)]_2$ at the MP4(SDQ) level predict activation energies for the two processes of 17.6 and 11.9 kcal/mol, respectively. Crystal data are as follows. $Ga(S\text{-}t\text{-}Bu)_3(HNMe_2)$, $C_{14}H_{34}GaNS_3$ at 223 K: $P2_1/n$ (monoclinic), $a = 9.6373(5)$ Å, $b = 12.7183(7)$ Å, $c = 16.9708(9)$ Å, $\beta = 91.9810(10)°$, and $Z = 4$. $[i\text{-}Pr_2NH_2][Ga(S\text{-}i\text{-}Pr)_4]$, $C_{18}H_{44}GaNS_4$ at 223 K: $P2_1/n$ (monoclinic), $a = 12.0179(6)$ Å, $b = 15.4813(8)$ Å, $c = 14.3875(8)$ Å, $\beta = 93.801(1)°$, and $Z = 4$. $[Ga(S\text{-}i\text{-}Pr)_3]_2$, $C_{18}H_{42}Ga_2S_6$ at 223 K: P-1(triclinic), $a = 8.6813(8)$ Å, $b = 9.2969(8)$ Å, $c = 11.1804(10)$ Å, $\alpha = 107.385(2)°$, $\beta = 95.987(1)°$, $\gamma = 117.285(1)°$, and $Z = 1$. $[Ga(S\text{-}t\text{-}Bu)_3]_2$, $C_{24}H_{54}Ga_2S_6$ at 223 K: $C2/c$ (monoclinic), $a = 10.0630(10)$ Å, $b = 17.698(2)$ Å, $c = 19.836(2)$ Å, $\beta = 98.500(10)°$, and $Z = 4$.

We are interested in using homoleptic gallium tris(*alkyl*thiolate) complexes as chemical vapor deposition precursors to sulfur-rich gallium sulfide and MGa_2S_4 (M = Ca, Ba, or Sr) films.[1−4] Compounds having *alkyl*thiolate ligands are of interest because they are potentially more volatile than compounds with arylthiolate ligands and the alkylthiolate C−S bond is weaker than in an arylthiolate, which may lead to cleaner decomposition during film deposition. There is ample precedent for using compounds with alkylthiolate ligands as chemical vapor deposition precursors to sulfide films.[5−9]

There are several reports in the literature concerning neutral homoleptic gallium alkylthiolate and arylthiolate compounds. One of the earliest was in 1965 by Funk and Paul, in which the synthesis of $Ga(SPh)_3$ from gallium metal and an excess of thiophenol is described.[10] Hoffmann later reported the synthesis of a series of $Ga(SR)_3$ compounds from reactions between $GaCl_3$ and Me_3SiSR (R = Me, Et, or Ph);[11] $GaPh_3$ and RSH (R = Me, Et, *n*-Pr, *i*-Pr, Ph or CH_2Ph);[12] and GaX_3 (X = Br or I) and $Pb(SR)_2$ (R = Me, Et, *n*-Pr, *i*-Pr, Ph or CH_2Ph).[13] In 1991, Ruhlandt-Senge and Power reported the synthesis and crystal structure of monomeric $Ga[S(2,4,6\text{-}t\text{-}Bu_3C_6H_2)]_3$, the only example of a structurally characterized homoleptic gallium tris(thiolate) complex.[14] Six-coordinate gallium tris(2-pyridinethiolate),[15,16] six-coordinate Ga(TS-TACN) (TS-TACN = the trithiolate ligand derived from 1,4,7-tris(2-mercaptoethyl)-1,4,7-triazacyclononane),[17] and the four-coordinate anions $[Ga(SR)_4]^-$ where R = Me, Et, *i*-Pr, Ph, 2,3,5,6-Me_4C_6H, or 2,4,6-$i\text{-}Pr_3C_6H_2$ have also been reported.[18]

In this paper, we report the synthesis and structures of two neutral homoleptic gallium alkylthiolates, $[Ga(SR)_2(\mu\text{-}SR)]_2$ (R = *i*-Pr or *t*-Bu), the salt $[i\text{-}Pr_2NH_2][Ga(S\text{-}i\text{-}Pr)_4]$, which is an intermediate in the synthesis of $[Ga(S\text{-}i\text{-}Pr)_2(\mu\text{-}S\text{-}i\text{-}Pr)]_2$, and the

[†] Department of Chemistry and Materials Research Science and Engineering Center.

[‡] Department of Chemistry.

(1) Schulz, S.; Gillan, E. G.; Ross, J. L.; Rogers, L. M.; Rogers, R. D.; Barron, A. R. *Organometallics* **1996**, *15*, 4880.
(2) Smith, D. C.; Samuels, J. A.; Espinoza, B. F.; Apen, E.; Peachey, N. M.; Dye, R. C.; Tuenge, R. T.; Schaus, C. F.; King, C. N. *Digest of 1995 SID Int. Symp.* **1995**, 728. The "Ga(S-*tert*-butyl)$_3$" mentioned in the Introduction section of this paper was intended to read "Ga(*tert*-butyl)$_3$": Smith, D. C. Personal communication.
(3) Djazovski, O. N.; Mikami, T.; Ohmi, K.; Tanaka, S.; Kobayashi, H. *J. Electrochem. Soc.* **1997**, *144*, 2159.
(4) Sun, S.-S.; Tuenge, R. T.; Kane, J.; Ling, M. *J. Electrochem. Soc.* **1994**, *141*, 2877.
(5) Bochmann, M.; Hawkins, I.; Willson, L. M. *J. Chem. Soc., Chem. Commun.* **1988**, 344.
(6) Cheon, J.; Gozum, J. E.; Girolami, G. S. *Chem. Mater.* **1997**, *9*, 1847.
(7) MacInnes, A. N.; Power, M. B.; Hepp, A. F.; Barron, A. R. *J. Organomet. Chem.* **1993**, *449*, 95.
(8) Barron, A. R. *Mater. Res. Soc. Symp. Proc.* **1994**, *335*, 317.
(9) Barron, A. R. *Adv. Mater. Opt. Electron.* **1995**, *5*, 245.
(10) Funk, H.; Paul, A. *Z. Anorg. Allg. Chem.* **1965**, *337*, 142.
(11) Hoffmann, G. G. *Chem. Ber.* **1983**, *116*, 3858.
(12) Hoffmann, G. G. *J. Organomet. Chem.* **1984**, *277*, 189.
(13) Hoffmann, G. G. *Chem. Ber.* **1985**, *118*, 1655.
(14) Ruhlandt-Senge, K.; Power, P. P. *Inorg. Chem.* **1991**, *30*, 2633.
(15) Rose, D. J.; Chang, Y. D.; Chen, Q.; Kettler, P. B.; Zubieta, J. *Inorg. Chem.* **1995**, *34*, 3973.
(16) Landry, C. C.; Hynes, A.; Barron, A. R. *Polyhedron* **1996**, *15*, 391.
(17) Moore, D. A.; Fanwick, P. E.; Welch, M. J. *Inorg. Chem.* **1990**, *29*, 672.
(18) Maelia, L. E.; Koch, S. A. *Inorg. Chem.* **1986**, *25*, 1896.

10.1021/ic981318j CCC: $18.00
Published on Web 03/19/1999

Lewis base adducts $Ga(SR)_3L$ (L = Me_2NH, R = *t*-Bu and L = py, R = *i*-Pr or *t*-Bu). Fluxional behavior exhibited by the $[Ga(SR)_2(\mu\text{-}SR)]_2$ compounds was studied by variable-temperature NMR and ab initio molecular orbital calculations.

Experimental Section

General Considerations. All manipulations were carried out in a glovebox or by using Schlenk techniques. Solvents were purified by using standard techniques after which they were stored in the glovebox over 4-Å molecular sieves. $GaCl_3$ was obtained from Strem and used without further purification, and the thiols were purchased from Aldrich and degassed before use. $[Ga(NMe_2)_3]_2$ was prepared by the literature method,[19] and $Ga(N\text{-}i\text{-}Pr_2)_3$, a pale yellow solid, was synthesized analogously from $GaCl_3$ and $LiN\text{-}i\text{-}Pr_2$ in a 1:1 mixture of ether and hexanes. NMR spectra were collected on a 300-MHz instrument. Elemental analyses were performed by Oneida Research Services (Whitesboro, NY).

Ga(S-*t*-Bu)$_3$(HNMe$_2$). *t*-BuSH (0.41 g, 4.5 mmol) was added dropwise to a solution of $[Ga(NMe_2)_3]_2$ (0.30 g, 0.74 mmol) in ether (10 mL). A white suspension formed that dissipated after the mixture was stirred for about 1 h. After an additional 1 h, the volatile components were removed from the reaction mixture in vacuo to give a white solid. The solid was dissolved in ether (~4 mL), and the flask was then placed in a freezer (−35 °C). After 18 h, colorless crystalline blocks had formed, which were isolated and dried in vacuo (yield 0.45 g, 80%). Anal. Calcd for $C_{14}H_{34}NS_3Ga$: C, 43.98; H, 8.96; N, 3.66. Found: C, 43.54; H, 8.66; N, 3.48. ^{1}H NMR (C_6D_6): δ 2.06 (d, 6, HN*Me*$_2$), 1.70 (s, 27, SC*Me*$_3$), 1.62 (br, 1, *H*NMe$_2$). $^{13}C\{^1H\}$ NMR (C_6D_6): 44.9 (s, 3, SC*Me*$_3$), 37.2 (s, 2, HN*Me*$_2$), 36.7 (s, 9, SC*Me*$_3$). IR (Nujol, KBr, cm^{-1}): ν(NH) 3208 m, 1398 w, 1362 s, 1269 w, 1211 w, 1155 s, 1115 w, 1044 m, 1020 m, 893 m, 818 w, 584 w.

[Ga(S-*t*-Bu)$_3$]$_2$. *t*-BuSH (0.21 g, 2.3 mmol) was added dropwise to a solution of $Ga(N\text{-}i\text{-}Pr_2)_3$ (0.28 g, 0.76 mmol) in ether (8 mL). About 10 min after the addition was complete, a white suspension began to form. After being stirred for a total of 2 h, the reaction mixture was taken to dryness in vacuo, leaving a white solid residue. An ^{1}H NMR spectrum of the residue showed that it was $[Ga(S\text{-}t\text{-}Bu)_3]_2$. The residue was extracted with toluene (1 × 30 mL), and the extract was filtered. The filtrate was concentrated in vacuo to ca. 10 mL, and the flask was placed in the freezer (−35 °C). After 15 h, colorless needles had formed that were isolated and dried in vacuo (yield 0.22 g, 86%). Anal. Calcd for $C_{24}H_{54}S_6Ga_2$: C, 42.73; H, 8.07. Found: C, 43.13; H, 8.10. ^{1}H NMR (C_6D_6): δ 1.72 (br s, 54, SC*Me*$_3$). $^{13}C\{^1H\}$ NMR (C_7H_8): 57.1 (s, 2, μ-SC*Me*$_3$), 47.1 (s, 4, SC*Me*$_3$), 36.7 (s, 12, SC*Me*$_3$), 34.7 (s, 6, μ-SC*Me*$_3$). IR (Nujol, KBr, cm^{-1}): 1364 m, 1213 m, 1155 s, 1024 w, 930 w, 818 m, 808 m, 577 m, 563m.

Ga(S-*t*-Bu)$_3$(py). Excess pyridine (0.42 g, 5.3 mmol) was added dropwise at room temperature to an ether (10 mL) solution of $[Ga(S\text{-}t\text{-}Bu)_3]_2$ (0.3 g, 0.45 mmol). After the mixture was stirred for 1 h, the ether and excess pyridine were removed in vacuo. The residue, a white solid, was dissolved in ether (~3 mL), and the flask was then placed in a freezer (−35 °C). After 15 h, colorless crystalline blocks had formed, which were isolated and dried in vacuo (yield 0.34 g, 92%). Anal. Calcd for $C_{17}H_{32}NS_3Ga$: C, 49.04; H, 7.75; N 3.36. Found: C, 49.08; H, 7.70; N, 3.17. ^{1}H NMR (C_6D_6): δ 9.18 (m, 2, *o*-py), 6.73 (m, 1, *p*-py), 6.45 (m, 2, *m*-py), 1.71 (s, 27, SC*Me*$_3$). $^{13}C\{^1H\}$ NMR (C_6D_6): 147.9 (2, *o*-py), 140.0 (1, *p*-py), 124.7 (2, *m*-py), 45.0 (s, 3, SC*Me*$_3$), 36.7 (s, 9, SC*Me*$_3$). IR (Nujol, KBr, cm^{-1}): 1607 m, 1485 m, 1450 s, 1362 s, 1213 m, 1167 s, 1150 s, 1063 m, 1044 m, 1015 m, 818 w, 766 s, 700 s, 640 m, 581 w.

[*i*-Pr$_2$NH$_2$][Ga(S-*i*-Pr)$_4$]. *i*-PrSH (0.62 g, 8.1 mmol) was added dropwise to a solution of $Ga(N\text{-}i\text{-}Pr_2)_3$ (0.30 g, 0.81 mmol) in ether (20 mL). After being stirred for a total of 18 h, the reaction mixture was taken to dryness under vacuum to give a white solid residue. The solid was extracted with ether (1 × 15 mL), and the extract was filtered. The filtrate was concentrated to ~5 mL, and the flask was placed in the freezer (−35 °C). After 13 h, colorless needles had formed, which were isolated and dried in vacuo (yield 0.35 g, 91%). Crystals suitable for an X-ray crystal structure determination were grown by dissolving the compound in hot toluene and then cooling the solution slowly to room temperature. Anal. Calcd for $C_{18}H_{44}NS_4Ga$: C, 45.75; H, 9.39; N, 2.96. Found: C, 45.71; H, 9.18; N, 2.72. ^{1}H NMR (CD_3CN): δ 6.13 (br, 2, H_2N-*i*-Pr$_2$), 3.45 (sept, 2, $^3J_{HH}$ = 6.3 Hz, N(C*H*Me$_2$)$_2$), 3.18 (sept, 4, $^3J_{HH}$ = 6.6 Hz, SC*H*Me$_2$), 1.25 (d, 24, $^3J_{HH}$ = 6.3 Hz, SCH*Me*$_2$), 1.27 (d, 12, $^3J_{HH}$ = 6.0 Hz, N(CH*Me*$_2$)$_2$). $^{13}C\{^1H\}$ NMR (C_6D_6): 48.4 (s, 2, N(*C*HMe$_2$)$_2$), 33.5 (s, 4, S*C*HMe$_2$), 29.4 (s, 8, SCH*Me*$_2$), 20.2 (s, 4, N(CH*Me*$_2$)$_2$). IR (Nujol, KBr, cm^{-1}): 2745 m, 2716 m, 2459 m, 2405 w, 2073 w, 1580 s, 1413 w, 1397 s, 1362 s, 1317 w, 1240 s, 1194 w, 1182 w, 1152 s, 1101 m, 1049 s, 976 w, 947m, 937 m, 887 m, 829 w, 627 s.

[Ga(S-*i*-Pr)$_3$]$_2$. Solid $[i\text{-}Pr_2NH_2][Ga(S\text{-}t\text{-}Bu)_4]$ (0.70 g, 1.5 mmol) was heated under vacuum (70 °C, 0.05 mmHg) to give a viscous oil. After being heated for 8 h, the oil was cooled to room temperature. During this time the oil solidified. The white solid was then sublimed (the solid again turned to a liquid) (85−95 °C, 0.05 mmHg) to give a white solid on the coldfinger (yield 0.28 g, 64%). Anal. Calcd for $C_{18}H_{42}S_6Ga_2$: C, 36.62; H, 7.17. Found: C, 36.11; H, 6.94. ^{1}H NMR ($CDCl_3$): δ 3.72 (br, 2, μ-SC*H*Me$_2$), 3.34 (br, 4, SC*H*Me$_2$), 1.41 (d, 36, $^3J_{HH}$ = 6.7 Hz, SCH*Me*$_2$). $^{13}C\{^1H\}$ NMR ($CDCl_3$): 39.8 (br, 2, μ-S*C*HMe$_2$), 33.9 (br, 4, S*C*HMe$_2$), 28.7 (br, 8, SCH*Me*$_2$), 26.0 (br, 4, μ-SCH*Me*$_2$). IR (Nujol, KBr, cm^{-1}): 1365 s, 1310 w, 1246 s, 1151 s, 1049 s, 930 m, 882 m, 619 s, 608 s.

Ga(S-*i*-Pr)$_3$(py). Excess pyridine (0.40 g, 5.1 mmol) was added dropwise to an ether (10 mL) solution of $[i\text{-}Pr_2NH_2][Ga(S\text{-}t\text{-}Bu)_4]$ (0.50 g, 1.1 mmol). After the solution was stirred overnight, the ether and excess pyridine were removed in vacuo to give a colorless viscous oil. The oil was extracted with hexanes (1 × 10 mL), and the extract was filtered through Celite. The filtrate was taken to dryness in vacuo to afford the adduct as a white powder (yield 0.38 g, 96%). Anal. Calcd for $C_{14}H_{26}NS_3Ga$: C, 44.93; H, 7.00; N 3.74. Found: C, 44.57; H, 6.88; N, 3.85. ^{1}H NMR (C_6D_6): δ 8.89 (m, 2, *o*-py), 6.60 (m, 1, *p*-py), 6.30 (m, 2, *m*-py), 3.66 (septet, 3, $^3J_{HH}$ = 6.6 Hz, SC*H*Me$_2$), 1.52 (d, 18, $^3J_{HH}$ = 6.6 Hz, SCH*Me*$_2$). $^{13}C\{^1H\}$ NMR (C_6D_6): 147.4 (2, *o*-py), 140.1 (1, *p*-py), 124.9 (2, *m*-py), 33.3 (s, 3, S*C*HMe$_2$), 29.3 (s, 6, SCH*Me*$_2$). IR (Nujol, KBr, cm^{-1}): 1609 m, 1453 s, 1364 m, 1252 m, 1215 m, 1152 m, 1068 m, 1045 m, 885 w, 694 m, 642 w, 623 w.

X-ray Crystallography. Crystal data are presented in Table 1. Crystals of Ga(S-*t*-Bu)$_3$(HNMe$_2$) and $[Ga(S\text{-}t\text{-}Bu)_3]_2$ are colorless prismatic blocks while $[Ga(S\text{-}i\text{-}Pr)_3]_2$ and $[i\text{-}Pr_2NH_2][Ga(S\text{-}i\text{-}Pr)_4]$ are colorless prismatic columns and colorless thick plates, respectively. The crystals were handled under mineral oil during the mounting procedures. Data were collected on Siemens SMART CCD (Ga(S-*t*-Bu)$_3$(HNMe$_2$), $[Ga(S\text{-}i\text{-}Pr)_3]_2$, and $[i\text{-}Pr_2NH_2][Ga(S\text{-}i\text{-}Pr)_4]$) and Siemens P4 ($[Ga(S\text{-}t\text{-}Bu)_3]_2$) instruments. No experimental difficulties were encountered. Two experimental items of note are as follows: The amine hydrogen of Ga(S-*t*-Bu)$_3$(HNMe$_2$) was located in a difference map and allowed to refine independently, and the C10/C11/C12 isopropyl group in $[(i\text{-}Pr)_2NH_2][Ga(S\text{-}i\text{-}Pr)_4]$ is disordered over two slightly different orientations having populations of approximately 50% each. Full details can be found in the Supporting Information.

Calculations. All calculations were carried out using the Gaussian94 package.[20] The geometries of the ground-state models C_{2h} *anti*-$[Ga(SH)_2(\mu\text{-}SH)]_2$ and C_s *syn*-$[Ga(SH)_2(\mu\text{-}SH)]_2$ (mirror plane perpendicular to Ga···Ga) and the transition states for the syn-to-anti conversion (maintaining C_s symmetry) and the terminal-bridge thiolate exchange (C_1) were fully optimized at the MP2 level using the frozen core approximation. The basis set used for these geometry optimizations was composed of the effective core potentials and corresponding valence double-ζ basis sets of Hay and Wadt for Ga and S[21] and the standard 3-21G basis for H.[22] The resulting geometries were confirmed as minima

(19) Nöth, H.; Konrad, P. Z. *Z. Naturforsh. B* **1975**, *30b*, 681.

(20) Gaussian 94 (Revision B.1): Frisch, M. J.; Trucks, G. W.; Schlegel, H. B.; Gill, P. M. W.; Johnson, B. G.; Robb, M. A.; Cheeseman, J. R.; Keith, T. A.; Petersson, G. A.; Montgomery, J. A.; Raghavachari, K.; Al-Laham, M. A.; Zakrzewski, V. G.; Ortiz, J. V.; Foresman, J. B.; Cioslowski, J.; Stefanov, B. B.; Nanayakkara, A.; Challacombe, M.; Peng, C. Y.; Ayala, P. Y.; Chen, W.; Wong, M. W.; Andres, J. L.; Replogle, E. S.; Gomperts, R.; Martin, R. L.; Fox, D. J.; Binkley, J. S.; Defrees, D. J.; Baker, J.; Stewart, J. P.; Head-Gordon, M.; Gonzalez, C.; Pople, J. A. Gaussian, Inc., Pittsburgh, PA, 1995.

Table 1. Crystal Data for $Ga(S\text{-}t\text{-}Bu)_3(HNMe_2)$, $[i\text{-}Pr_2NH_2][Ga(S\text{-}i\text{-}Pr)_4]$, $[Ga(S\text{-}i\text{-}Pr)_3]_2$, and $[Ga(S\text{-}t\text{-}Bu)_3]_2$

compound	$Ga(S\text{-}t\text{-}Bu)_3(HNMe_2)$	$[i\text{-}Pr_2NH_2][Ga(S\text{-}i\text{-}Pr)_4]$	$[Ga(S\text{-}i\text{-}Pr)_3]_2$	$[Ga(S\text{-}t\text{-}Bu)_3]_2$
formula	$C_{14}H_{34}GaNS_3$	$C_{18}H_{44}GaNS_4$	$C_{18}H_{42}Ga_2S_6$	$C_{24}H_{54}Ga_2S_6$
fw	382.32	472.50	590.32	674.47
crystal dimens (mm)	0.40 × 0.35 × 0.35	0.45 × 0.20 × 0.20	0.15 × 0.15 × 0.12	0.40 × 0.30 × 0.25
space group	$P2_1/n$ (monoclinic)	$P2_1/n$ (monoclinic)	$P\bar{1}$ (triclinic)	$C2/c$ (monoclinic)
a, Å	9.6373(5)	12.0179(6)	8.6813(8)	10.0630(10)
b, Å	12.7183(7)	15.4813(8)	9.2969(8)	17.698(2)
c, Å	16.9708(9)	14.3875(8)	11.1804(10)	19.836(2)
α, deg	90.00	90.00	107.385(2)	90.00
β, deg	91.9810(10)	93.801(1)	95.987(1)	98.500(10)
γ, deg	90.00	90.00	117.285(1)	90.00
T, °C	−50(2)	−50(2)	−50(2)	−50(2)
Z	4	4	1	4
V, Å^3	2078.87(19)	2670.9(2)	733.71(11)	3493.9(6)
D_{calcd}, g/cm^3	1.22	1.18	1.34	1.28
μ, mm^{-1}	1.616	1.345	2.266	1.912
R, R_w[a]	0.017, 0.044[b]	0.023, 0.058[c]	0.021, 0.055[d]	0.027, 0.075[e]

[a] $R = \sum||F_o| - |F_c||/\sum|F_o|$; $R_w = [\sum w(F_o^2 - F_c^2)^2/\sum w(F_o^2)^2]^{1/2}$. [b] $w = [\sigma^2(F_o^2) + (0.0205P)^2 + (0.6670P)]^{-1}$ where $P = (F_o^2 + 2F_c^2)/3$. [c] $w = [\sigma^2(F_o^2) + (0.0239P)^2 + (1.3861P)]^{-1}$ where $P = (F_o^2 + 2F_c^2)/3$. [d] $w = [\sigma^2(F_o^2) + (0.0232P)^2 + (0.3964P)]^{-1}$ where $P = (F_o^2 + 2F_c^2)/3$. [e] $w = [\sigma^2(F_o^2) + (0.0355P)^2 + (8.9292P)]^{-1}$ where $P = (F_o^2 + 2F_c^2)/3$.

or transition-state structures via numerical frequency calculations. Higher level single-point energy calculations of the optimized structures were then undertaken at the frozen core MP4(SDQ) level with a larger basis set generated by adding a set of d-polarization functions[21] on Ga (exponent = 0.185) and S (exponent = 0.503) to the basis previously described and converting the basis on H to the standard 6-31G** set.[22] The energies resulting from these calculations were then corrected for zero-point vibrational energies using the calculated corrections obtained from the respective frequency calculations performed at the MP2 level. The total energies and geometrical details of each stationary point are available from the authors upon request.

Results and Discussion

Synthesis. A summary of our synthetic results is presented in Scheme 1.

The amide complex $[Ga(NMe_2)_3]_2$ reacts with excess *t*-BuSH in ether to give a suspension that eventually dissolves. Workup of the reaction mixture and crystallization from ether affords $Ga(S\text{-}t\text{-}Bu)_3(HNMe_2)$ in 80% yield. The white suspended material initially formed in the reaction is probably the salt $[Me_2NH_2][Ga(S\text{-}t\text{-}Bu)_4]$, which either reacts further with unreacted $GaNMe_2$-containing species or decomposes to give the final product (see below). The coordinated amine could not be removed from $Ga(S\text{-}t\text{-}Bu)_3(HNMe_2)$ by heating the compound in vacuo (75 °C, 0.05 mmHg) or by dissolving it in CH_2Cl_2 and then vacuum distilling the solvent.

With the preparation of $Ga(S\text{-}t\text{-}Bu)_3(HNMe_2)$ in hand, the gallium amide complex $Ga(N\text{-}i\text{-}Pr_2)_3$ was synthesized for reaction with *t*-BuSH. It was assumed that *i*-Pr_2NH, because of its bulkiness, would be not coordinate to $Ga(S\text{-}t\text{-}Bu)_3$ as strongly as Me_2NH and this, in turn, would allow formation of the homoleptic thiolate. This proved to be correct; $Ga(N\text{-}i\text{-}Pr_2)_3$ reacts with excess *t*-BuSH to give moderately soluble $[Ga(S\text{-}t\text{-}Bu)_3]_2$ in high yield. The crude reaction product, after being held under dynamic vacuum for 12 h, was examined by NMR and showed no evidence for the presence of the amine adduct. An attempt to sublime $[Ga(S\text{-}t\text{-}Bu)_3]_2$ under vacuum resulted in decomposition.

Scheme 1

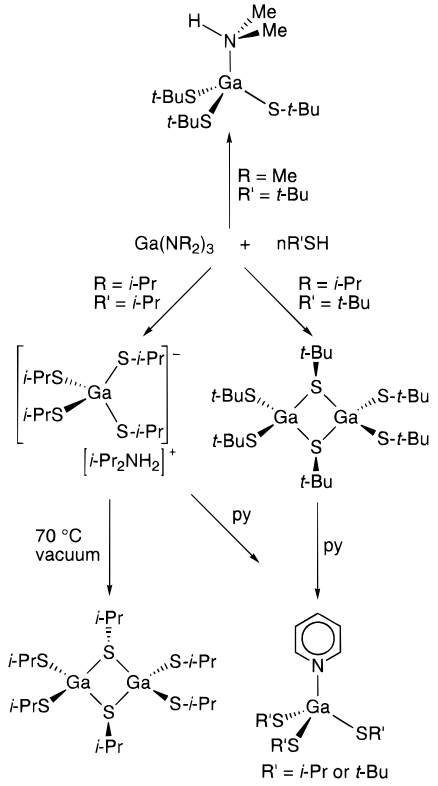

In contrast to the reaction with *t*-BuSH, $Ga(N\text{-}i\text{-}Pr_2)_3$ reacts with excess *i*-PrSH to give the salt $[i\text{-}Pr_2NH_2][Ga(S\text{-}i\text{-}Pr)_4]$, which can be isolated as crystalline colorless needles from hot toluene. Prolonged heating of the salt in vacuo (70 °C, 0.05 mmHg) causes formation of an oil that solidifies upon cooling to room temperature. Sublimation from the solid (85−90 °C, 0.05 mmHg) produces the neutral homoleptic compound $[Ga(S\text{-}i\text{-}Pr)_3]_2$ on the coldfinger as a white solid in moderate yield. The compound can crystallized as colorless thick plates from a mixture of hexanes and toluene. In contrast to these results, in two previous literature reports "$Ga(S\text{-}i\text{-}Pr)_3$" was said to be a colorless oil.[12,13]

The thermal decomposition of $[i\text{-}Pr_2NH_2][Ga(S\text{-}i\text{-}Pr)_4]$ to give $[Ga(S\text{-}i\text{-}Pr)_3]_2$ indicates that amine and thiol were lost from the salt. To test whether a similar process could occur in solution, an ether solution of $[i\text{-}Pr_2NH_2][Ga(S\text{-}i\text{-}Pr)_4]$ was treated with

(21) Wadt, W. R.; Hay, P. J. *J. Chem. Phys.* **1985**, *82*, 284. Höllwarth, A.; Böhme, M.; Dapprich, S.; Ehlers, A. W.; Gobbi, A.; Jonas, V.; Köhler, K. F.; Stegmann, R.; Veldkamp, A.; Frenking, G. *Chem. Phys. Lett.* **1993**, *208*, 237.

(22) Binkley, J. S.; Pople, J. A.; Hehre, W. J. *J. Am. Chem. Soc.* **1980**, *102*, 939. Hariharan, P. C.; Pople, J. A. *Theor. Chim. Acta* **1973**, *28*, 213.

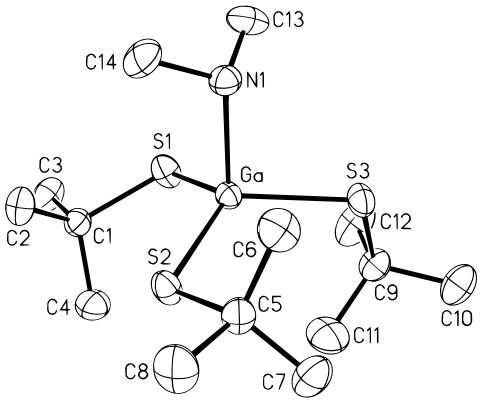

Figure 1. View of the Ga(S-*t*-Bu)$_3$(HNMe$_2$) molecule showing the atom numbering scheme. Thermal ellipsoids are 40% equiprobability envelopes, with hydrogens omitted.

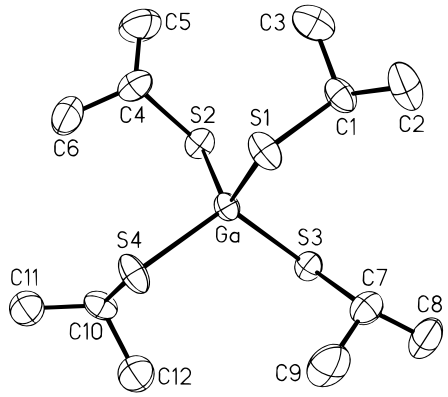

Figure 2. View of the anion in [*i*-Pr$_2$NH$_2$][Ga(S-*i*-Pr)$_4$] showing the atom numbering scheme. Thermal ellipsoids are 40% equiprobability envelopes, with hydrogens omitted.

excess pyridine. This procedure gave the neutral adduct Ga(S-*i*-Pr)$_3$(py) in nearly quantitative yield, suggesting a possible equilibrium in solution involving the salt, HN-*i*-Pr$_2$, *i*-PrSH, and "Ga(S-*i*-Pr)$_3$." In the reaction with pyridine, the initial formation of [pyH][Ga(S-*i*-Pr)$_4$] and HN-*i*-Pr$_2$ can be excluded because HN-*i*-Pr$_2$ is more basic than pyridine (cf. pK_a(H$_2$N-*i*-Pr$_2$) $\approx$ 11.0 at 28.5 °C and pK_a(pyH) $\approx$ 5.3 at 25 °C).[23] The *tert*-butylthiolate analogue of Ga(S-*i*-Pr)$_3$(py) is formed in nearly quantitative yield by reacting pyridine with [Ga(S-*t*-Bu)$_3$]$_2$.

X-ray Crystallographic Studies. The X-ray crystal structures of Ga(S-*t*-Bu)$_3$(HNMe$_2$) (Figure 1), [*i*-Pr$_2$NH$_2$][Ga(S-*i*-Pr)$_4$] (Figure 2), [Ga(S-*i*-Pr)$_3$]$_2$ (Figure 3) and [Ga(S-*t*-Bu)$_3$]$_2$ (Figure 4) were determined. Selected bond distances and angles are presented in Table 2. Full details can be found in the Supporting Information.

The structure of Ga(S-*t*-Bu)$_3$(HNMe$_2$) resembles In(S-*t*-Bu)$_3$(py).[24] Molecules of Ga(S-*t*-Bu)$_3$(HNMe$_2$) can be described as trigonal pyramidal with the HNMe$_2$ occupying the apical position. The gallium and three sulfur atoms are nearly planar (Σ(S−Ga−S) = 348°) with the Ga atom lying 0.46 Å out of the plane defined by the sulfur atoms. In In(S-*t*-Bu)$_3$(py), for comparison, the three S−In−S angles sum to 351°.[24]

The anion in the salt [(*i*-Pr)$_2$NH$_2$][Ga(S-*i*-Pr)$_4$] has a distorted tetrahedral geometry that is similar to those of the anions in [*i*-Pr$_4$N][Ga(SEt)$_4$] and [Et$_4$N][Ga(SPh)$_4$].[18] In the GaS$_4$ core of [Ga(S-*i*-Pr)$_4$]$^-$ the S−Ga−S angles vary from 97 to 118°.

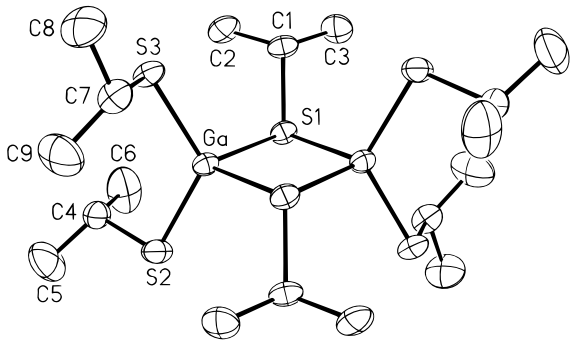

Figure 3. View of the [Ga(S-*i*-Pr)$_3$]$_2$ molecule showing the atom numbering scheme. Thermal ellipsoids are 40% equiprobability envelopes, with hydrogens omitted.

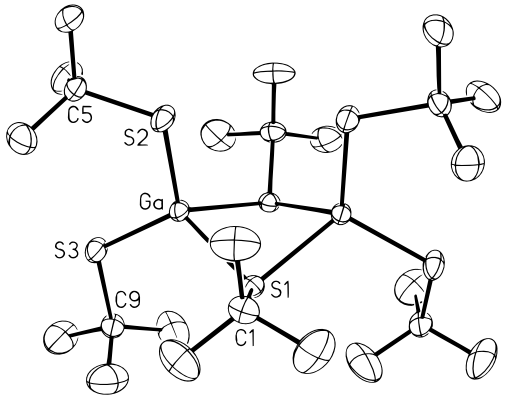

Figure 4. View of the [Ga(S-*t*-Bu)$_3$]$_2$ molecule showing the atom numbering scheme. Thermal ellipsoids are 40% equiprobability envelopes, with hydrogens omitted.

The angles at gallium in [Ga(SPh)$_4$]$^-$ fall in a narrower range, 100 to 115°, while those in [Ga(SEt)$_4$]$^-$ are all ~109°.[18] In the solid, the cation [(*i*-Pr)$_2$NH$_2$]$^+$ is associated with the [Ga(S-*i*-Pr)$_4$]$^-$ anions via N−H···S hydrogen bonding (Figure 5). The hydrogen bonding makes two of the Ga−S bonds (S3 and S4) slightly longer (by ~0.02 Å) than the other two are.

The Ga(SR)$_3$ (R = *i*-Pr and *t*-Bu) compounds are dimers with two bridging thiolate ligands. The coordination geometries at the gallium atoms can be described as distorted tetrahedral. Molecules of [Ga(S-*i*-Pr)$_3$]$_2$ are centrosymmetric with the central core consisting of a planar *anti*-Ga(μ-SR)$_2$Ga four-membered ring. A planar *anti*-Ga(μ-SR)$_2$Ga core was also found in [I$_2$Ga(μ-SMe)]$_2$,[25] [Ph$_2$Ga(μ-SEt)]$_2$,[26] [Ph$_2$Ga(μ-SSnCy$_3$)]$_2$,[27] [*t*-Bu$_2$Ga(μ-SH)]$_2$,[28] and [Et$_2$Ga(μ-SSiPh$_3$)]$_2$.[29] Molecules of [Ga(S-*t*-Bu)$_3$]$_2$ are slightly different. They have crystallographic 2-fold symmetry, and the central core is a *syn*-Ga(μ-SR)$_2$Ga four-membered ring with a butterfly-type structure similar to the one found in [I$_2$Ga(μ-S-*i*-Pr)]$_2$.[30] Compounds with butterfly *anti*-Ga(μ-SR)$_2$Ga four-membered rings, such as [(PhCH$_2$)$_2$Ga(μ-S-*t*-Bu)]$_2$ and [Me$_2$Ga(μ-SC$_6$F$_5$)]$_2$,[31,32] have also been structurally characterized. The fold angle along the Ga···Ga′ vector in [Ga-

(23) *CRC Handbook of Chemistry and Physics*; Weast, R. C., Ed.; CRC Press: Cleveland, 1974.
(24) Suh, S.; Hoffman, D. M. *Inorg. Chem.* **1998**, *37*, 5823.
(25) Boardman, A.; Jeffs, S. E.; Small, R. W. H.; Worrall, I. J. *Inorg. Chim. Acta* **1985**, *99*, L39.
(26) Hoffmann, G. G.; Burschka, C. *J. Organomet. Chem.* **1984**, *267*, 229.
(27) Ghazi, S. U.; Heeg, M. J.; Oliver, J. P. *Inorg. Chem.* **1994**, *33*, 4517.
(28) Power, M. B.; Barron, A. R. *J. Chem. Soc., Chem. Commun.* **1991**, 1315.
(29) Beachely, Jr., O. T.; Rosenblum, D. B.; Churchill, M. R.; Lake, C. H.; Toomey, L. M. *Organometallics* **1996**, *15*, 3653.
(30) Hoffmann, G. G.; Burschka, C. *Angew. Chem., Int. Ed. Engl.* **1985**, *24*, 970.
(31) Kopp, M. R.; Neumüller, B. *Z. Anorg. Allg. Chem.* **1997**, *623*, 796.
(32) Hendershot, D. G.; Kumar, R.; Barber, M.; Oliver, J. P. *Organometallics* **1991**, *10*, 1917.

Table 2. Selected Bond Distances (Å) and Angles (deg) for $Ga(S\text{-}t\text{-}Bu)_3(HNMe_2)$, $[i\text{-}Pr_2NH_2][Ga(S\text{-}i\text{-}Pr)_4]$, $[Ga(S\text{-}i\text{-}Pr)_3]_2$, and $[Ga(S\text{-}t\text{-}Bu)_3]_2$

compound	$Ga(S\text{-}t\text{-}Bu)_3(HNMe_2)$	$[i\text{-}Pr_2NH_2][Ga(S\text{-}i\text{-}Pr)_4]$	$[Ga(S\text{-}i\text{-}Pr)_3]_2$	$[Ga(S\text{-}t\text{-}Bu)_3]_2$
		Distances		
Ga−S1	2.2477(5)	2.2541(6)	2.3799(6)	2.3614((9)
Ga−S2	2.2402(5)	2.2583(6)	2.2106(7)	2.2255(10)
Ga−S3	2.2649(4)	2.2796(6)	2.2188(6)	2.2208(10)
Ga−S4		2.2791(6)		
Ga−S1′			2.3611(6)	2.3961(10)
Ga−N1	2.0758(14)			
avg (range)	1.86	1.83	1.85	1.85
C−S	(1.848(16)−1.8608(17))	(1.826(2)−1.837(2))	(1.838(3)−1.860(2))	(1.844(4)−1.869(4))
		Angles		
S1−Ga−S2	115.117(17)	118.22(2)	110.07(2)	111.32(4)
S1−Ga−S3	113.393(18)	113.99(2)	108.47(2)	117.66(4)
S1−Ga−S4		100.91(2)		
S2−Ga−S3	119.264(18)	97.10(2)	122.33(3)	117.14(4)
S1−Ga−S1′			95.07(2)	79.26(4)
S2−Ga−S4		113.11(2)		
S2−Ga−S1′			108.33(2)	112.18(4)
S3−Ga−S4		114.35(2)		
S3−Ga−S1′			109.13(2)	113.45(4)
Ga−S−Ga			84.93(2)	88.80(3)
N1−Ga−S1	100.56(5)			
N1−Ga−S2	107.88(4)			
N1−Ga−S3	96.60(4)			
$\Sigma(X\text{−}S_{bridge}\text{−}Y)$			301	323
avg (range)	109.5	104.3	104.5	114.2
Ga−S−C	(108.35(6)−111.08(6))	102.63(7)−105.79(8)	101.00(9)−108.12(8)	110.05(12)−118.20(13)

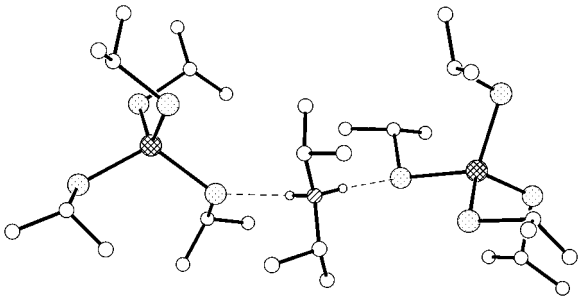

Figure 5. Ball-and-stick plot of $[i\text{-}Pr_2NH_2][Ga(S\text{-}i\text{-}Pr)_4]$ showing the N−H···S hydrogen bonding between $[(i\text{-}Pr)_2NH_2]^+$ and $[Ga(S\text{-}i\text{-}Pr)_4]^-$.

$(S\text{-}t\text{-}Bu)_3]_2$ is 126.4°, which can be compared to 143° and 152° for the same angles in $[I_2Ga(\mu\text{-}S\text{-}i\text{-}Pr)]_2$[30] and $[Me_2Ga(\mu\text{-}SC_6F_5)]_2$,[32] respectively, and the angle between the GaS_2 planes is 130.6°. The three-coordinate bridging sulfur atom in $[Ga(S\text{-}t\text{-}Bu)_3]_2$ is flattened ($\Sigma(X\text{−}S1\text{−}Y) = 323°$) compared to $[Ga(S\text{-}i\text{-}Pr)_3]_3$ ($\Sigma(X\text{−}S1\text{−}Y) = 301°$). The flattening at the sulfur bridge may be related to the bulk of the sulfur substituent; for example, compare $[Et_2Ga(\mu\text{-}SSiPh_3)]_2$ ($\Sigma(X\text{−}S_{bridge}\text{−}Y) = 331°$),[29] $[(PhCH_2)_2Ga(\mu\text{-}S\text{-}t\text{-}Bu)]_2$ (avg 317°)[31] and $[Ph_2Ga(\mu\text{-}SSnCy_3)]_2$ (313°)[27] to those in $[Ph_2Ga(\mu\text{-}SEt)]_2$ (295°),[26] $[Me_2Ga(\mu\text{-}SC_6F_5)]_2$ (avg 304°),[32] $[Me_2Ga(\mu\text{-}SC_5H_9)]_2$ (300°),[33] and $[Ph_2Ga(\mu\text{-}SC_5H_9)]_2$ (298°).[33] The Ga−S1 and Ga−S1′ distances within the four-membered rings of the $[Ga(SR)_3]_3$ compounds differ only slightly.

The terminal Ga−S distances in $Ga(S\text{-}t\text{-}Bu)_3(HNMe_2)$, $[Ga(S\text{-}t\text{-}Bu)_3]_2$, $[i\text{-}Pr_2NH_2][Ga(S\text{-}i\text{-}Pr)_4]$, and $[Ga(S\text{-}i\text{-}Pr)_3]_2$ range from 2.21 to 2.28 Å, with the shortest distances found in the dimers. These can be compared to the terminal distances in $Ga[S(2,4,6\text{-}t\text{-}Bu_3C_6H_2)]_3$ (avg 2.205(1) Å),[14] Mes^*_2GaSMe ($Mes^* = 2,4,6\text{-}t\text{-}Bu_3C_6H_2$; 2.271(2) Å), *n*-$BuGa(SMes^*)_2$ (avg 2.211(9) Å),[34] $[i\text{-}Pr_4N][Ga(SEt)_4]$ (2.264(3) Å), and $[Et_4N][Ga(SPh)_4]$ (2.257(3) Å).[18] The Ga−S_{bridge} bond distances (2.3611(6)−2.3961(10) Å) in $[Ga(SR)_2(\mu\text{-}SR)]_2$ (R = *t*-Bu or *i*-Pr) fall within the range of Ga−S_{bridge} distances reported for $[X_2Ga(\mu\text{-}SR)]_2$ compounds where X = iodide, alkyl, or aryl (2.327(3)−2.460(2) Å).[25−33]

NMR Observations for $[Ga(SR)_3]_2$ Compounds. Assuming $[Ga(S\text{-}i\text{-}Pr)_3]_2$ adopts a solution structure with virtual C_{2h} symmetry similar to the one observed in the solid state, its limiting ^1H NMR spectrum should consist of three doublets of equal intensity, one doublet arising from the bridging ligands and two from the terminal ligands, and two septets in a 2:1 ratio (the septet of intensity 2 may be misshapen because of coupling to two inequivalent methyl groups). Similarly, the limiting $^{13}C\{^1H\}$ NMR spectrum should consist of five singlets, three arising from the thiolate methyl groups and two from the methine carbons. The molecule $[Ga(S\text{-}t\text{-}Bu)_3]_2$ has virtual C_{2v} symmetry in the solid state. Its ^1H and $^{13}C\{^1H\}$ limiting spectra should consist of three equally intense singlets and six singlets, respectively. In fact, both $[Ga(SR)_3]_2$ compounds exhibit fluxional behavior in solution and in neither case could limiting spectra be obtained that are consistent with the solid-state structures.

The ^1H NMR spectrum of $[Ga(S\text{-}i\text{-}Pr)_3]_2$ recorded at room temperature (toluene-d_8) consists of a sharp doublet in the methyl region and broad hump in the methine region (Figure 6). As the temperature is lowered to 0 °C, the broad methine resonance separates to two broad resonances and the methyl doublet broadens. On cooling to −20 °C, a spectrum is produced consisting of two methyl doublets (2:1) and two methine septets (2:1). Similar spectra are observed at lower temperatures (to −90 °C) except that at very low temperatures there is some broadening of all the resonances due to the increase in solvent viscosity. Temperature-dependent carbon-13 spectra are observed as well. The $^{13}C\{^1H\}$ spectra recorded at room temperature, for example, consist of three broad resonances, but at 0 °C and below (to −60 °C) four well-resolved singlets (at 0 °C: 39.9, 34.0 (*C*HMe_2) and 28.9, 25.6 (CH*Me*$_2$)) are observed.

The ^1H NMR spectrum of $[Ga(S\text{-}t\text{-}Bu)_3]_2$ in toluene-d_8 at room temperature consists of only one singlet, but in $CDCl_3$ solution two singlets in a 2:1 ratio, which are assigned to

(33) Unpublished results quoted in ref 27.
(34) Wehmschulte, R. J.; Ruhlandt-Senge, K.; Power, P. P. *Inorg. Chem.* **1995**, *34*, 2593.

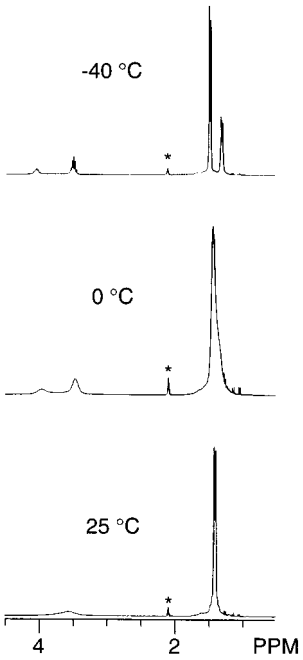

Figure 6. Proton NMR spectra recorded at three temperatures for a toluene-d_8 solution of $[Ga(S\text{-}i\text{-}Pr)_3]_2$. The peak labeled with the * arises from the solvent.

terminal and bridge thiolate ligands, respectively, are observed. This indicates the lone singlet observed in the spectrum of the toluene-d_8 solution is the result of an accidental degeneracy. The accidental degeneracy is lifted upon cooling the sample to 10 °C and below (to −40 °C) because of slight changes in chemical shifts with temperature. The two singlets remain sharp and unchanged in the 10 to −40 °C temperature range. Room-temperature $^{13}C\{^1H\}$ NMR spectra (toluene-d_8) are consistent with the ^1H spectra in that four singlets are observed, arising from bridge (57 (CMe_3) and 35 (CMe_3) ppm) and terminal (47 and 37 ppm) thiolate ligands. Carbon-13 NMR spectra recorded at temperatures above room temperature, however, indicate that $[Ga(S\text{-}t\text{-}Bu)_3]_2$ exhibits fluxional behavior similar to $[Ga(S\text{-}i\text{-}Pr)_3]_2$. At 40 °C, for example, the four sharp peaks observed at room temperature are broad with the peak at 57 ppm barely visible in the baseline. At 60 °C, the highest temperature examined, the tertiary carbon resonances collapse completely into the baseline and the methyl carbon resonances merge into one broad resonance.

Possible Explanations for the NMR Observations. The temperature-dependent NMR spectra observed for the $[Ga(SR)_3]_2$ compounds can be explained by two fluxional processes, a high energy process ($\Delta G^{\ddagger} \approx 14$ kcal/mol (*i*-Pr) and 16 kcal/mol (*t*-Bu))[35] involving bridge-terminal thiolate ligand exchange and a low energy process, which was not frozen out in either case, that is effectively inversion at sulfur. It is the latter process that makes the observed low-temperature limiting spectra appear as though the $[Ga(SR)_3]_2$ molecules have virtual D_{2h} symmetry rather than C_{2h} (R = *i*-Pr) or C_{2v} (R = *t*-Bu) symmetry in solution. In the case of $[Ga(S\text{-}t\text{-}Bu)_3]_2$, the possibility the molecule adopts a solution *anti*-$Ga(\mu\text{-}S\text{-}t\text{-}Bu)_2Ga$ structure having virtual C_{2h} symmetry (akin to the one observed for $[Ga(S\text{-}i\text{-}Pr)_3]_2$ in the solid state) cannot be excluded since a limiting C_{2h} structure for $[Ga(S\text{-}t\text{-}Bu)_3]_2$ would be consistent with its observed room-temperature NMR spectra.

Scheme 2

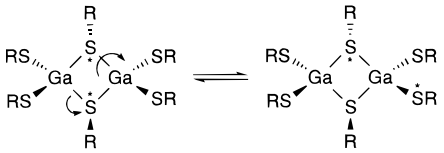

Scheme 3

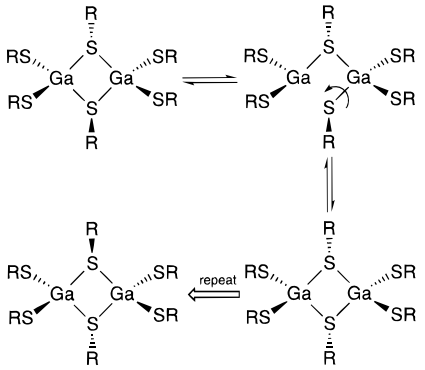

The bridge-terminal exchange mechanism may involve simply moving the bridging thiolate ligands to terminal positions while simultaneously moving two terminal thiolates to the bridge positions but it is difficult to imagine what would hold the $Ga(SR)_3$ fragments together in the transition state. Alternatively, the bridge-terminal exchange could occur by the mechanism shown in Scheme 2, where one $Ga-S_{bridge}$ bond is broken at a time and the bond breaking is accompanied by rotation about the $Ga'-S'_{bridge}$ bond. A dimer−monomer equilibrium is another possibility, but an argument against it is that the activation energy for bridge-terminal exchange in the *tert*-butylthiolate derivative is higher than in the isopropylthiolate derivative when the opposite would be expected.

The lower energy S_{bridge} inversion fluxional process could be an umbrella-like inversion at the three-coordinate sulfur or, alternatively, one in which a $Ga-S_{bridge}$ bond breaks and there is rotation about the new $Ga-S_{terminal}$ bond (Scheme 3). The mechanism shown in Scheme 3 is analogous to a pathway proposed to account for syn−anti isomerization in $[Me_2Ga(\mu\text{-}NH\text{-}t\text{-}Bu)]_2$.[36]

Molecular Orbital Calculations. Ab initio molecular orbital calculations were used to probe the dynamic processes. A calculation at the MP4(SDQ) level on $[Ga(SH)_2(\mu\text{-}SH)]_2$ gives the syn isomer to be 0.1 kcal/mol more stable than the anti geometry. To model the mechanism in Scheme 2, one $Ga-S_{bridge}$ bond in $[Ga(SH)_2(\mu\text{-}SH)]_2$ was broken and the $Ga(SH)_3$ fragment in the four-coordinate GaS_4 moiety was rotated about the remaining $Ga-S_{bridge}$ bond by 60°. Upon optimization, a transition state was found (**I**) that has an activation energy of 17.6 kcal/mol with respect to the syn ground state. This is close to the estimated value for syn−anti exchange obtained from the variable-temperature NMR data. One of the $Ga-S_{bridge}$ bonds in the transition state is computed to be quite long, 2.78 Å, which is 0.30 Å longer than the Ga−S bridging distances found in the syn and anti structures. In fact, the binding energy of two optimized $Ga(SH)_3$ monomers relative to the syn ground state was 18.6 kcal/mol (including superpositon error), indicating the transition state for bridge-terminal exchange is very close to the dissociation limit.

(35) Martin, M. L.; Delpuech, J.-J.; Martin, G. J. *Practical NMR Spectroscopy*; Heyden: Philadelphia, 1980; Chapter 8.1.2.

(36) Park, J. T.; Kim, Y.; Kim, J.; Kim, K.; Kim, Y. *Organometallics* **1992**, *11*, 3320.

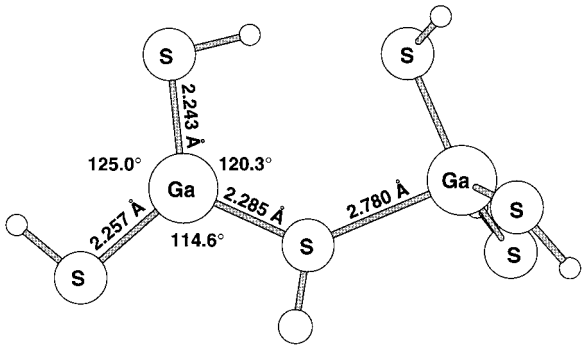

I

The umbrella inversion at the three-coordinate sulfur in SH_3^+ is a high-energy process (~30 kcal/mol) according to our calculations and those carried out previously.[37] This would seem to suggest that inversion at the three-coordinate S_{bridge} atoms in the $[Ga(SR)_3]_2$ molecules should similarly be a high-energy process.[38] Calculations at the MP4(SDQ) level show, however, that the barrier to inversion at S_{bridge} in $[Ga(SH)_2(\mu\text{-}SH)]_2$ is only 12.0 kcal/mol relative to the syn ground state. The lower than expected energy for the umbrella inversion is due to stabilization of the trigonal planar sulfur transition state by an S pπ to Ga−S σ^* interaction, shown schematically in **II**.

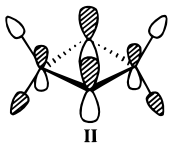

II

Consistent with this explanation, the calculated Ga−S distances involving the planar S_{bridge} atom were found to be shorter (2.43 Å) than those involving the pyramidal S_{bridge} atom (2.48 Å).

To probe the alternative sulfur inversion mechanism shown in Scheme 3, two possible transition states having structures similar to the $(RS)_2Ga(\mu\text{-}SR)Ga(SR)_3$ structure shown in Scheme 3 were investigated. In one case, the Ga−SH bond was rotated counterclockwise (i.e., as shown in Scheme 3) to bring the hydrogen substituent into the Ga_2SS_{bridge} plane. Optimization of this structure resulted in dissociation to a pair of $Ga(SH)_3$ monomers. Similarly, the Ga−S bond was rotated clockwise to bring the hydrogen substituent into the Ga_2SS_{bridge} plane. Optimization in this case resulted in a collapse of the structure to the transition state for the umbrella inversion. Thus, on the basis of the calculations, the more likely mechanism for inversion at sulfur in the dimers is the simple umbrella mechanism.

Conclusion

The thiol *t*-BuSH reacts with $[Ga(NMe_2)_3]_2$ to give the amine adduct $Ga(S\text{-}t\text{-}Bu)_3(HNMe_2)$ and with the new bulky amide complex $Ga(N\text{-}i\text{-}Pr_2)_3$ to give the dimer $[Ga(S\text{-}t\text{-}Bu)_3]_2$. In contrast to the latter reaction, $Ga(N\text{-}i\text{-}Pr_2)_3$ reacts with *i*-PrSH to afford the salt $[i\text{-}Pr_2NH_2][Ga(S\text{-}i\text{-}Pr)_4]$, which loses amine and thiol on heating under vacuum to give the dimer $[Ga(S\text{-}i\text{-}Pr)_3]_2$. The salt also loses amine and thiol in solution when it is reacted with excess pyridine, yielding the adduct $Ga(S\text{-}i\text{-}Pr)_3(py)$. The analogous pyridine adduct $Ga(S\text{-}t\text{-}Bu)_3(py)$ is prepared by reacting $[Ga(S\text{-}t\text{-}Bu)_3]_2$ with pyridine. X-ray crystallographic studies show that the homoleptic thiolate compounds have $[Ga(SR)_2(\mu\text{-}SR)]_2$ structures in the solid state with planar anti (R = *i*-Pr) and butterfly syn (R = *t*-Bu) $Ga(\mu\text{-}SR)_2Ga$ four-membered rings and that the gallium centers in $Ga(S\text{-}t\text{-}Bu)_3(HNMe_2)$ and $[i\text{-}Pr_2NH_2][Ga(S\text{-}i\text{-}Pr)_4]$ have trigonal-pyramidal and distorted tetrahedral geometries, respectively. The dimers exhibit fluxional behavior involving two separate processes, effective inversion at the bridging sulfur atoms and a higher energy bridge-terminal thiolate ligand exchange. For the former process, an umbrella-like S_{bridge} inversion mechanism is consistent with both variable-temperature NMR data and the results of molecular orbital calculations that were used to probe the dynamic processes. The bridge-terminal ligand exchange mechanism is less clear, but a bond-breaking/bond-rotation mechanism is most consistent with the data.

Our purpose in preparing gallium alkylthiolate complexes was to identify potential chemical vapor deposition precursors to sulfur-rich gallium sulfide and MGa_2S_4 (M = Ca, Ba, or Sr) films. Of the new compounds, $[Ga(S\text{-}i\text{-}Pr)_3]_2$ appears to be the most promising candidate because of its volatility and thermal stability. Film deposition studies using $[Ga(S\text{-}i\text{-}Pr)_3]_2$ as a precursor and the preparation of analogous liquid compounds that would be better suited for use in conventional chemical vapor deposition precursor delivery systems are underway.

Acknowledgment for technical assistance with the crystal structure determinations is made to Dr. James Korp. This work was supported in part by the Robert A. Welch Foundation, by the MRSEC Program of the National Science Foundation under Award No. DMR-9632667, and by the State of Texas through the Texas Center for Superconductivity at the University of Houston and the Advanced Research Program.

Supporting Information Available: Four X-ray crystallographic files, in CIF format. This material is available free of charge via the Internet at http://pubs.acs.org.

IC981318J

(37) Roszak, S.; Strasburger, K.; Chojnacki, H. *J. Mol. Struct.* **1991**, *227*, 187.

(38) An excellent review on the stereodynamics of metal complexes of sulfur-, selenium-, and tellurium-containing ligands has been published: Abel, E. W.; Orrell, K. G.; Bhargava, S. K. *Prog. Inorg. Chem.* **1984**, *32*, 1.

(39) Inversion barriers are sensitive to polarization functions added to the basis set and not so heavily on correlation techniques. For SH_3^+, which was used as a benchmark for this study, the inversion barrier (with the large basis set identified in the Experimental Section) was found to be 29.0 [MP2], 29.1 [MP4(SDQ)], 29.3 [QCISD], and 29.4 kcal/mol [QCISD(T)]. On this basis, the computations at the MP4(SDQ) level are expected to be reliable.